Nanoscale

ARTICLE

Synthesis of 1D-Glyconanomaterials by a Hybrid Noncovalent-Covalent Functionalization of Single Wall Carbon Nanotubes: Study of their Selective Interactions with Lectins and with Live Cells.

Received 00th January 20xx,
Accepted 00th January 20xx

DOI: 10.1039/x0xx00000x

www.rsc.org/

M. Pernía Leal, [a] M. Assali,[a] J. J. Cid, [a] V. Valdivia,[a,b] J. M. Franco, [c,d] I. Fernández,[b] D. Pozo,[c,d] N. Khiar. [a,]*

To take full advantage of the remarkable applications of carbon nanotubes in different fields, there is a need to develop effective methods to improve their water dispersion and biocompatibility while maintaining their physical properties. In this sense, current approaches suffer from serious drawbacks such as loss of electronic structure together with low surface coverage in the case of covalent functionalizations, or instability of the dynamic hybrids obtained by non-covalent functionalizations. In the present work, we examined the molecular basis of an original strategy that combines the advantages of both functionalizations without their main drawbacks. Hierarchical self-assembly of diacetylenic-based neoglycolipids into highly organized and compacted rings around the nanotubes, followed by photopolymerization leads to the formation of nanotubes covered with glyconanorings with a shish kebab-type topology exposing the carbohydrate ligands to the water phase in a multivalent fashion. The glyconanotubes obtained are fully functional, able to establish specific interactions with their cognate receptors. In fact, by taking advantage of this selective binding, an easy method to sense lectins as a working model of toxin detection was developed based on a simple analysis of TEM images. Remarkably, different experimental settings to assess cell membrane integrity, cell growth kinetics and cell cycle demonstrated the cellular biocompatibility of the sugar-coated carbon nanotubes compared to pristine single-walled carbon nanotubes.

1 Introduction.

Single-walled carbon nanotubes (SWCNTs) are interesting 1D nanomaterials endowed with unique size shape and physical properties that are currently being actively investigated in different fields,[1-4] with some important applications already in the market.[5,6] The discovery that SWCNTs can be internalized within cells[7,8] has opened the door for their application in the nascent field of nanomedicine.[9-14] Currently CNTs are being actively investigated as nanovectors for smart delivery of cytotoxic drugs,[15-19] nucleic acids[20-22] or proteins,[23,24] as ultra-sensitive biosensors,[25-27] in tumor therapy by thermal ablation, or as nanocomposite materials for tissue engineering.[28-30] However, the controversial CNT toxicity still remains a concern, mainly as a consequence of lack of common standards,[31] contradictory results or non-comprehensive studies reported in the literature.[32-41] Besides, length and surface chemistry of CNTs strongly influence their cytotoxicity profiles,[42] and therefore their biocompatibility may be engineerable.[43-45] Thus, the set-up of efficient methods for the synthesis of biocompatible water soluble SWCNTs is an important preliminary requirement for their clinical applications. While covalent[46-48] and non-covalent[49-51] approaches have been applied for the dispersion of SWCNTs in aqueous media, both methods have limitations that hinder the fully exploitation of the exceptional potential of CNTs. Covalent functionalizations, for instance, provide robust and stable aggregates, but generally take place with low surface coverage in addition to a disruption of the π-network, leading to losses in their mechanical, electrical, and biosensing properties.[4] Conversely, the non-covalent functionalization approach is most desirable as it takes place generally with high surface coverage, do not affect the surface of CNTs, and maintained their physical properties unaltered. Carbohydrates, as bioactive poly-hydroxylated compounds have been widely used to enhance water solubility and biocompatibility of carbon nanotubes without compromising their sensing capabilities.[55-56] However, the resulting aggregates may lack long-term stabilities as a consequence of the weak nature

[a] Asymmetric Synthesis and Functional Nanosystems Group. Instituto de Investigaciones Químicas (IIQ), CSIC and Universidad de Sevilla, C/ Américo Vespucio 49, 41092, Seville (Spain). E-mail: khiar@iiq.csic.es
[b] Departamento de Química Orgánica y Farmacéutica, Universidad de Sevilla, C/ García González 2, 41012 Seville (Spain).
[c] Advanced Therapies in Neuroprotection and Immune Regulation Laboratory. Andalusian Center for Molecular Biology and Regenerative Medicine (CABIMER), Av. Americo Vespucio s/n, 41092, Seville (Spain).
[d] Department of Medical Biochemistry, Molecular Biology and Immunology, University of Seville, Av. Sanchez Pizjuan s/n, 41009, Seville (Spain).

†Electronic Supplementary Information (ESI) available: [Experimental procedures for the synthesis of compounds **12-10, 12-15, 17-20, 22-25, 27-30,** NMR spectra, and additional TEM images]. See DOI: 10.1039/x0xx00000x

the forces involved in the assembly and their dynamic nature, increasing the risk of uncontrolled defunctionalisation within the cells. Thus, the development of a hybrid strategy which combines the advantages of both approaches with a particular focus on potential biological applications is highly desirable.[57-58] Though, a possible solution could be the use of pre-programed self-assembling monomers which can be further manipulated in the supramolecular state in order to endow the nano-assemblies with the sought physicochemical stability.[59-61] Diacetylenic amphiphiles are well suited for such purpose, as they can undergo topochemical reactions upon UV-irradiation or thermal stimuli, leading to the anisotropic formation of poly(diacetylene) (PDA) in the crystalline state.[52-64] Closely packed and properly ordered diacetylenes amphiphiles undergo a smooth and clean photo-polymerization *via* 1,4-addition reaction, affording functional PDA nanomaterials with enhanced stability and interesting chromatic properties.[65-68] These exceptional physico-chemical properties have boosted the utilization of diacetylenic amphiphiles as self-organizing monomers for the synthesis of various functional nanostructured materials, among them liposomes,[69] micelles,[70] films,[71] and lipid nanotubes,[72] mainly, for *in vitro* sensing applications, although available data regarding cellular biocompatibility remain scarce.

Using diacetylenic based glycolipids as responsive su organizing monomers in water, we have recently reported different methods for the synthesis various multivalen glyconanosystems with different sizes and topologies.[69,73-76] A distinct feature of the above approaches is that they rely o molecularly defined, monodispersed building blocks well suited for chemical tailoring and library generation. Takin advantage of this, in the current work, we have studied the scope of the hierarchical self-organization of diacetyleni based glycolipids on nanotube sidewalls as an accurate hybrid chemical (covalent) and physical (noncovalent) method for the biofunctionalization of SWCNTs with cellular compatibility profiles including the effects on cell cycle as an essential ste for their biological applications, Figure 1. The glyconanotube obtained are fully functional, able to establish specifi interactions with their cognate receptors. Moreover, th particular shish kebab topology of the final nanoconstru allows the development of a simple method for the selective detection of lectins as working model of toxins by TEM anal

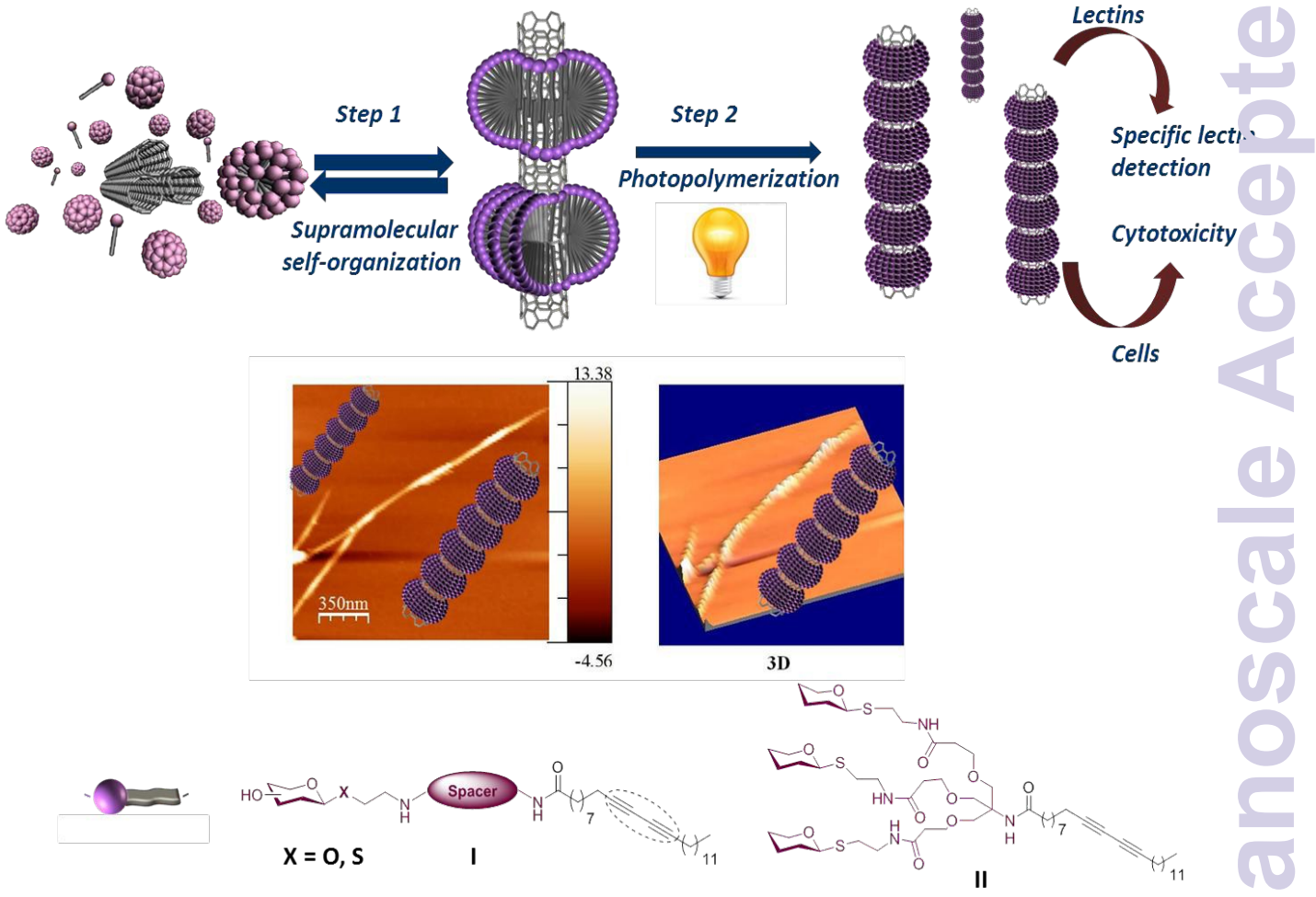

Figure 1. Synthesis and applications of hierarchically self-assembled and photopolymerized neoglycolipids onto SWCNTs sidewall reported in this work.

Nanoscale

ARTICLE

2 Results and discussion

2.1 Chemistry

2.1.1. Synthesis of linear diacetylenic-based glycolipid

While a number of amphiphilic molecules have been used to the exfoliation of carbon nanotubes,[77-79] a full understanding of the mechanism for dispersing CNTs with surfactants is still lacking.[80-82] The accumulated results show that the success of the dispersion rests on tail-tail and tail-nanotube hydrophobic interaction, and is highly dependent on the concentration and structure of the surfactant.[83-85] In order to unravel the structural requirement of the diacetylenic glycolipids for an optimal hierarchical self-association on CNTs sidewall, a set of different *S*- and *O*-glycolipids with linear sugar head groups (compound **I**, Figure 1) or dendritic structure (compound **II**, Figure 1) were designed. The linear glycolipids (**I**), Figure 1, contain a monovalent functional glycoligand head group tethered to a variable hydrophilic linker for adjusting the hydrophilic/hydrophobic balance of the molecule, and a 25 carbon-based hydrophobic tail included for efficient Van der Waals interactions with the CNT sidewalls bearing, furthermore, the desired photo-polymerizable diacetylenic function. As bioactive sugar head groups, we chose to work with lactose and mannose because of their relevant biological activities. In this sense, alterations in glycosylation patterns, which have been observed for all types of malignant cells, usually result in increased exposure of terminal galactose,[86-87] while mannose oligosaccharides are ubiquitous in cells infection by toxins and pathogens such as bacteria, HIV and Ebola viruses among others.[88-92]

In a preliminary work, we have used thioglycosides[74] as mimics of natural *O*-glycoside, easy to synthesize, and resistant toward glycosidases.[93-96] A convergent synthetic approach has been developed for the synthesis of neoglycolipids with different hydrophilic-hydrophobic balance (**3-6)**, in two or four steps starting from 2-aminoethyl thioglycosides **1** or **2,** Figure 2.

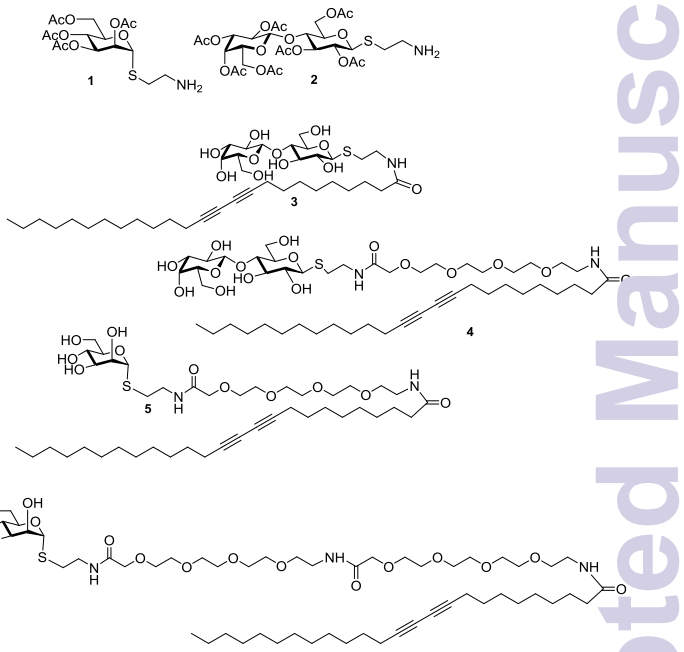

Figure 2: Structures of (2-aminoethyl)-2,3,4,6,-tetra-*O*-acetyl-1-thio-α-D-mannoside 1 and (2-aminoethyl)-2,2′,3,3′,4′,6,6′-hepta-*O*-acetyl-1-thio-β-D-lactoside 2 used in the synthesis of functional S-linked neoglycolipids 3-6.

Herein, we directed our attention to the synthesis of the more challenging diacetylenic-based neoglycolipids with natural *O*-glycosides. In the case of mannose tethered neoglycolipids, the synthesis of the required (2-aminoethyl)-2,3,4,6,-tetra-*O*-acetyl-α-mannoside **10** was performed from (2-azidoethyl)-2,3,4,6,-tetra-*O*-acetyl-α-mannoside **9**. Although this compound is usually obtained in two steps, glycosidation of mannose pentaacetate **7** with 2-chloroetanol followed by nucleophilic displacement of the chloride by the azide,[97] we have found that the direct glycosidation using 2-azidoethanol[98] **8** as glycosyl acceptor and borontrifluoride etherate as catalyst rendered the desired compound in reasonable yield, Scheme 1. Reduction of **8** in presence of H_2 and Pd/C gave the corresponding amine **10** in quantitative yield. The amide bond formation between the compound **10** and the bifunctional spacer **11**, gave the corresponding azide derivative **12** in 73% yield. The reduction in presence of H_2-Pd/C and the following amide coupling with the pentacosadiinoic acid (PCDA) gave the desired *O*-glycolipid **14** in good yield. A Zemplen deacetylation[99] led to the *O*-mannoside derivative **15** in quantitative yield, Scheme 1.

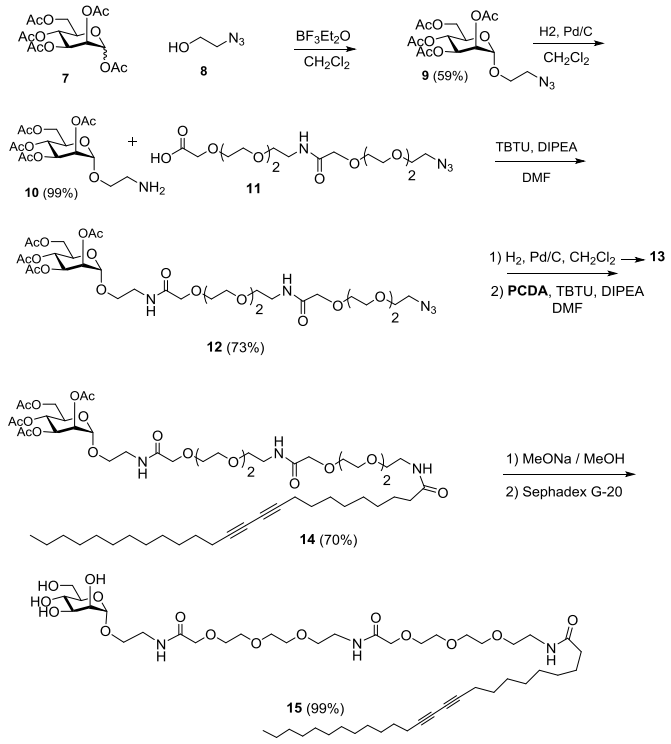

Scheme 1. Synthesis of diacetylenic-based neoglycolipid with α-D-mannopyranoside head group **15**

In the case of the neoglycolipid with a lactose head group, the synthesis of the desired 2-(azidoethyl)lactose heptaacetate did not take place when starting from lactose octaacetate **16** as glycosyl donor, highlighting that a more reactive glycosyl donor was needed. Compound **19** was, then, prepared from the trichloroacetimidate **18**, obtained in two steps from lactose octaacetate **16**.[100] The first step is the selective deprotection at the anomeric position with hydrazine acetate in DMF giving the corresponding lactol **17** in 86% yield, Scheme 2. The addition of trichloroacetonitrile under basic conditions in methylene chloride gave the glycosyl donor **18** in an excellent yield.[101] The glycosylation reaction using the trichloroacetimidate **18** in presence of $BF_3{\cdot}Et_2O$ and the glycosyl acceptor **8** afforded the β-lactoside **19** in 45% yield. Finally, the reduction of **19** with H_2 and Pd/C gave the desired amine **20** in a quantitative yield, Scheme 2. Next, as in the case of the mannose-based neoglycolipid, amide bond formation between the compound **20** and the spacer **21** gave the corresponding azide derivative **22** in 86% yield. The reduction in presence of H_2-Pd/C (→ **23**) and the following amide coupling with the PCDA gave the desired *O*-glycolipid **24** in good yield. A Zemplen deacetylation led to the *O*-mannoside derivative lipid **25** in quantitative yield, Scheme 2.

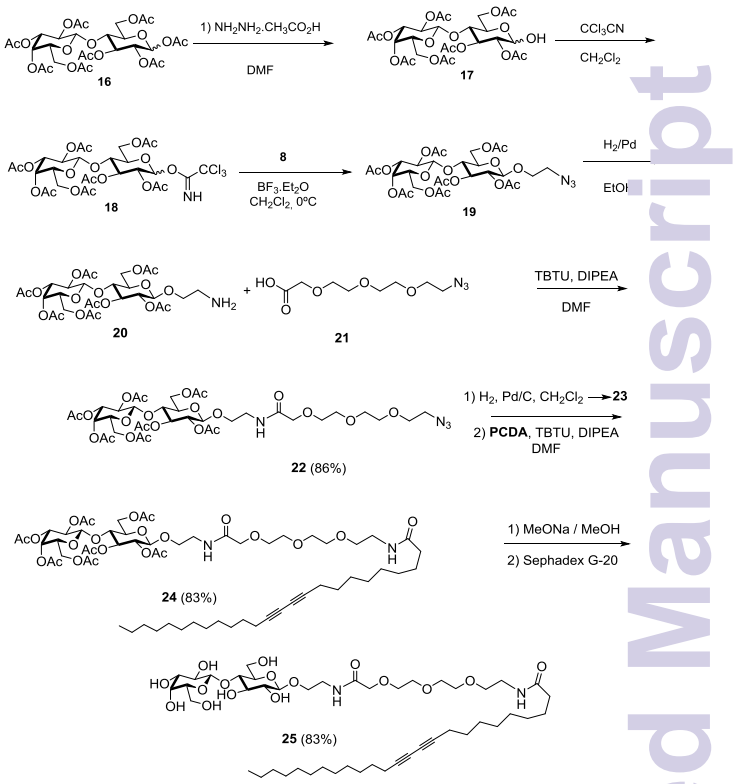

Scheme 2. Synthesis of diacetylenic-based neoglycolipid with lactose head group **25.**

2.1.2 Synthesis of the glycodendritic lipid

The next design made to the biofunctionalization and water dispersion of CNTs was based on the use of glycodendrimers as homogenous bioactive coating. In addition to various biomedical applications,[102-104] dendrimers have been used to encapsulate metal nanoparticle catalysts,[105] to functionalize CNTs with bioactive compounds for DNA sensing,[106] cancer targeting and imaging.[107]

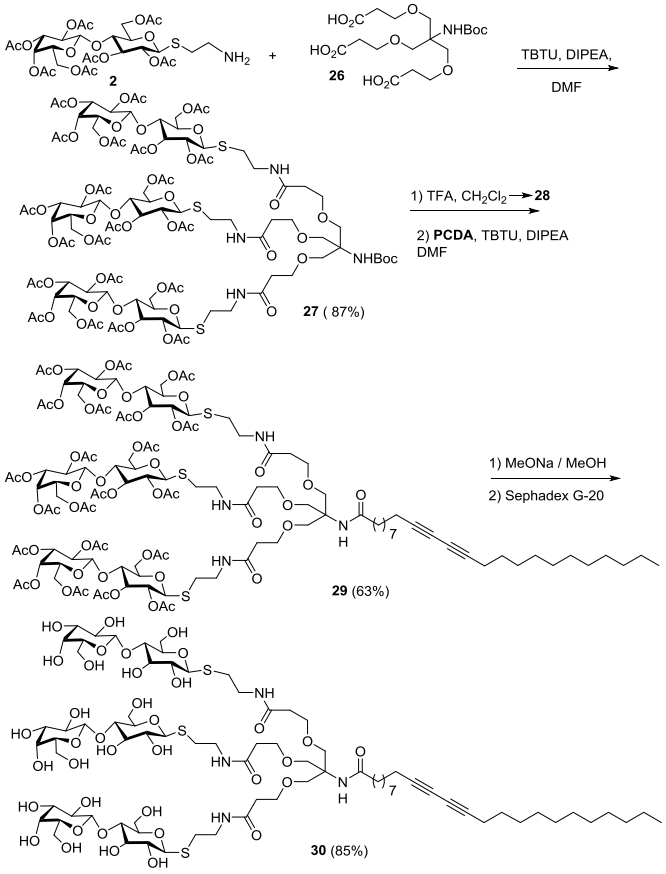

Scheme 3. Synthesis of lactose-based dendritic glycolipid **30**

The proposed strategy is based on the synthesis of a dendritic glycolipid **II** (Figure 2), where the polar head consists of three copies of a carbohydrate. The dendritic core **26** of this glycolipid, was synthesised in four steps from the tris(hydroxymetyl)aminomethane as described in the literature.[108] The amide bond formation between the amino derivative β-lactose **2** and **26** using TBTU, DIPEA in DMF gave the glycodendron **27** in 87% yield. Deprotection of the amine group of compound **27** with trifluoroacetic acid (TFA), and reaction of the obtained amine **28** with PCDA afforded the diacetylenic glycolipid **29** in 67% yield. Finally, a Zemplen deacetylation gave the dendritic glycolipid **30** in 85% yield (Scheme 2).

The spectroscopic and analytical data for the free linear **3-6**, **15**, **25** and the dendritic neoglycolipids **30,** used for the solubilization studies of CNTs, are consistent with their molecular structure.

2.2.Studies on the water dispersion of SWCNTs

Pristine nanotubes form dense bundles and ropes containing hundreds of close-packed CNTs, tightly entangled characterized by van-der-Waals attraction energies of 50 eV μm^{-1}. To overcome the energy of this interaction and disperse CNTs in water, the most widely used method consists in the sonication of CNTs in the presence of a dispersant.[109] Exfoliation of individual nanotubes from their bundles by a surfactant is postulated to occur through an 'unzippering' mechanism,[110] whereby the ultrasonic agitation produces gaps between adjacent nanotubes at the end of a bundle, allowing surfactant molecules to adsorb onto the newly exposed surface. Surfactant adsorption propagates along the fissure, eventually splitting the bundle or separating an individual nanotube from the aggregate.

We thus conducted the exfoliation study of SWCNTs by sonicating during 30 min a mixture of 1 mg of the neoglycolipid in 1 mL of deionized water. Initially, sonication of the nanotubes in the presence of homogeneous aqueous solution of **3** afforded unstable aggregates as evidenced by the rapid precipitation of the nanotubes after a few minutes in the medium. On the contrary, mixing the more hydrophilic neutral lipid **4** with SWCNTs, afforded a black solution that remained stable for months. Similar stable black suspension was obtained when lactose-based *O*-glycolipid **15** was used with SWCNTs. These results highlight the importance of the hydrophilic spacer, indicating that an increase of the hydrophilic-hydrophobic balance of the glycolipids is mandatory for the functionalization of SWNTs and to maintain the individualized tubes stable. This observation is doubly corroborated by the results obtained with mannose-coated neoglycolipids **5, 6** and **15**. On the one hand, the decrease of the hydrophilic/hydrophobic balance of the surfactant by using a monosaccharide-based glycolipid **5** gave exclusively unstable aggregates that precipitated quickly in water. On the other hand, enhancing the hydrophilicity of the molecule by using a longer polyoxygenated spacer in **6** and **15**, afforded a stable aggregate and the formation of a black solution which remained stable for months.

Surprisingly, sonication of SWCNTs in the presence of homogeneous aqueous solution of dendritic glycolipid **30** afforded unstable aggregates and the subsequent precipitation of the SWCNTs in water. A possible explanation for this unexpected result could be that the presence of a large polar head group impedes glycodendron **30** to self-organise properly in hemimicelles around the nanotube surface by steric hindrance (*vide infra*), causing nanotube depletion and precipitation.

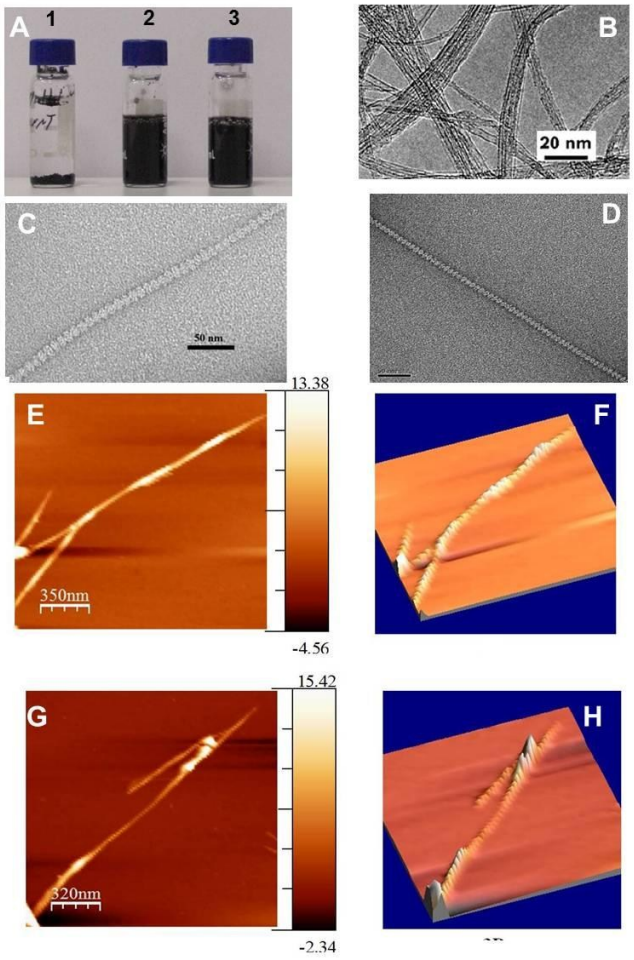

Figure 3. A) Photographs of vials containing pristine SWCNT (1), glyconanotubes SWCNT-**4** and SWCNT-**6** (3). TEM image of as produced SWCNTs (B), glyconanotubes SWCNT-**4** (C) and SWCNT-**6** (D). Bi-dimensional (E) and tridimensional (F) AFM images of SWCNTs-**4**. Bi-dimensional (G) and tridimensional (H) AFM images of SWCNTs-**6**

Summarizing, the previous studies highlight that in order to disperse the nanotubes, diacetylenic based neoglycolipids must be linear with a monovalent sugar head group, and an adequate hydrophilic/hydrophobic balance. To achieve that, an oxygenated chain derived from tetratehylene glycol is sufficient in the cases where the hydrophilic head group is a disaccharide (**4**, and **25**), while in the case of monosacharides (**6** and **15**) it is necessary to double the length of the oxygenated spacer.

2.3.Characterization of the aggregates

The characterization of SWCNT-neoglycolipid aggregates was firstly carried out by TEM and AFM analysis. The TEM analysis, which represents the best method for the direct visualization of neoglycolipids-coated carbon nanotubes, has been done by deposition of 20 μL of the mixture on honey carbon grids. After 1 min, the applied solution was removed from the grid with a filter paper, and the grid was negatively stained with a 2% uranyl acetate solution for 1 min. The TEM grids were examined using a Philips CM-200 TEM operating at an accelerating voltage of 200 keV and magnifications of 10000-300000 times. AFM images were obtained by the trapping mode of a water-solution drop of the glyconanotubes on a j exfoliated mica plate using a Pico Plus Molecular Imagin microscope.

TEM images of native SWCNTs and SWCNTs-coated with lactose-based glycolipid (SWCNTs-**4)** and SWCNTs-coated wit mannose (SWCNTs-**6**) are given in Figure 4B, 4C, and 4D, respectively. As indicated before, due to the hydrophob interactions, van-der-Waals forces, and π-stacking among individual tubes, as produced SWCNTs usually exist as dens bundles or rope that are deeply interconnected in a 3D manner, Figure 3B. Quite outstandingly, simple functionalization with neoglycolipids **4, 6**, **15**, and **25** in pur water and strictly neutral conditions, allowed the SWCNT packages to exfoliate producing small, mainly individual, suga coated nanotubes, as evidenced by TEM (3C, 3D) as well as b 2D- and 3D-AFM analysis (Figure 3E, 3F, 3G, and 3H, se additional figures in supporting information).

Interestingly, the TEM images show that the complete surface of the nanotube is covered by striations as pearls on an o necklace. Moreover, AFM (specially the AFM-3D image) of glyconanotubes SWCNT-**4** (Figure 3E and 3F), and SWCN (Figure 3G and 3H) corroborated the shish-kebab topology o the nanoconstructs, reflecting consecutive striations on the tube surfaces, as a consequence of the supramolecular sel organization of the neoglycolipids on the nanotube surface.

Despite the large number of experimental and theoretical studies of surfactant-CNTs interactions, no consensus has bee reached on the arrangements of the amphiphilic molecules on the nanotube surface at the molecular level.[111-114] The cumulative data using small-angle neutron scattering (SANS) and TEM experiments led to the propositions of three sel assembly models: "random adsorption",[115] "cylindrical micelles",[116-117] and "hemimicelle".[118-119] The regular striation along the nanotube surface observed in TEM, and especially in 2D- and 3D-AFM images reported for the first time herein as well as their dimensions rule out the cylindrical micelles and the random adsorption models and support the hemimicelar model. Moreover, we have observed that in order that the neoglycolipid self-organize in the hemimicellar manner on th CNT side wall, it is necessary to work with neogycoli concentration over its critical micelar concentration (4 μM fo neoglycolipid **4**, and 3.50 μM for neoglycolipid **6**). These data together with the spherical micelles observed in TEM image of the unpurified aggregates suggest that firstly th neoglycolipids form micelles in water before hierarchically self organizing onto the nanotube surface. An importan consequence of the hemimicelar model is that the self assembled neoglycolipids are closely packed and proper ordered to undertake the polymerization step onto the carbon nanotube side wall.

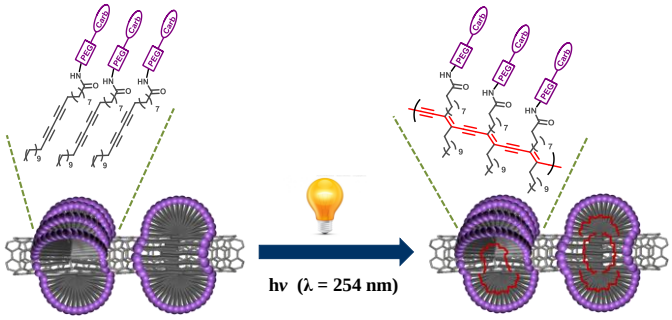

Figure 4. Polymerization of the glyconanorings-coated carbon nanotubes

Indeed, it is well documented that under such supramolecular organization, *i.e* in micelles and liposomes, the diacetylene lipids undergo easy and clean polymerization *via* 1,4-addition reaction leading alterning ene-yne polymer chains upon irradiation with 254 nm light.[64-68] In this particular case, the formation of the polymer chain will rigidify the inner core of each hemi micelle affording strong polymerized glyconanorings around the nanotube with shish kebab-like topologies, Figure 4.

Thus, after sonication of SWCNTs in the presence of aqueous solution of lipid **4** or lipid **6**, as before, the mixture was irradiated by a simple laboratory UV lamp (254 nm) for 12h. A first centrifugation at 825 x g allows the elimination of sediments of non-functionalized SWCNT and other impurities such as amorphous carbon and catalysts, and a second centrifugation at higher speed (17968 x g) allows the sedimentation of the functionalized SWCNT-neoglycolipids, which also permits the elimination of excess of lipids and micelles in the supernatant solution. The high stability of the polymerized glyconanotubes was ascertained by comparison with that of the non-polymerized counterpart. While the latter precipitated after three months, the former ones remained stable for years. Additionally, the suspension of polymerized glyconanotubes remained unchanged after washing with methanol, heating in water at 80ºC for one week, and when diluted in different buffers, in contrast with the non-polymerized CNT-glycolipids aggregates and to most of surfactant based CNT-solubilization systems developed so far.[120-121] These results clearly indicate that, as predicted, the SWCNT's are coated with polymerized glyconanorings, forming stable water soluble multicomposites. Although this assembly between the neoglycolipids and SWCNTs could be considered as a single entity, and not a dynamic equilibrium between both reactants, it was demonstrated that the glyconanorings were attached in a non-covalent manner without perturbing the π-network structure of carbon nanotubes by UV-Vis/NIR and Raman spectroscopy analysis.

UV-Vis/NIR absorbance spectra of the aggregates SWCNTs-**4** and SWCNTs-**6** present the characteristic peaks corresponding to the first and second pair of van Hove singularities bands (Figure 5A), indicating the good dispertion and the preservation of the electronic structure of the carbon nanotubes.[122-123] In this sense, it has been reported[124] that covalent modification the CNTs results in a disruption of the aromatic system which, in turn causes a change in the relat intensities of van Hove singularities. To further confirm thes results, a characterisation of the aggregates was carried ou using Raman spectroscopy at an excitation wavelength of 63 nm. Both spectra (blue and red curve in Figure 5B) presente an identical Raman spectrum than the bare SWCNTs (black curve in Figure 5B) with bands around 1580 cm^{-1} (G ban attributed to C-C sp^2 bonds from the aromatic structure of the SWCNT sidewalls.

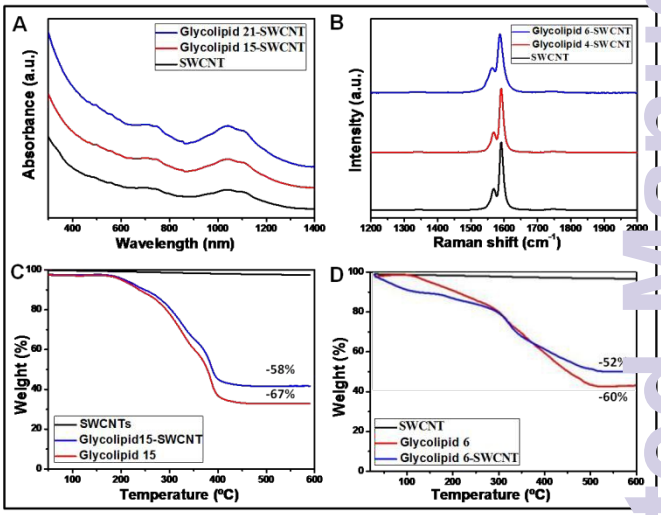

Figure 5. A) UV-Vis-NIR spectra of unfunctionalized SWCNT, and aggregate SWCNT-**4** and SWCNT-**6**. B) Raman spectra of unfunctionalized SWCNT, and aggregates SWCNT-**4** and SWCNT-**6**. Thermogravimetric analysis aggregates SWCNT-**4** (C) and SWCNT-**6** (D), and their corresponding glycolipids

The absence of a D-band around~1350 cm^{-1} characteristic of C-C sp^3 bonds, confirmed the absence of amorphous carbon defects on the aromatic structure of the carbon nanotubes.[125] The anthrone-sulfuric acid colorimetric assay was used determine the content of sugars in the glyconanotubes. Calibration curves were constructed based on the various lactose and mannose concentrations and their corresponding absorbance determined by spectrophotometer at 628 nm Then the concentrations of sugars within the aggregates w calculated from the calibration curves via their absorbances a 628 nm (see S.I.). A 29% of D-lactose and 40% of D-mannos were found in the aggregates SWCNTs-**4** and SWCNTs-**6** respectively, thus indicating a total percentage of 80% (0.8 mmol/g) and 87% (2.25 mmol/g) of their corresponding glycolipids. Additionally, and to confirm the results quantification by the anthrone method, we studied the weigh loss by thermogravimetric analysis (TGA). The percentage mass loss of SWNTs- **4** and SWNTs-**6** at 600°C (under a stream of N_2 at a heating rate of 20°C / min) was 58% and 52% respectively (Figure 5C and 5D). This loss is correlated with the stability of the starting glycolipids **4** and **6** at 600ºC, for whic the decrease in mass was 67% and 60%, respectively. Given these values, the total mass loss was estimated to be 87% and 86% for glycolipids **4** and **6** respectively, in agreement with

anthrone results. The described data confirms that we succeeded in developing a mixed method for the functionalization and dispersion of SWCNTs in water. Indeed, the obtained nanomaterials are highly stable and prevent their desorption in a biological medium, while the nanotube surface is totally covered by the neoglycolipids and maintains its electronic characteristics.

2.4 Lectin Binding Assays

The obtained glyconanotubes are covered by a dense carbohydrate array, and can be used as synthetic multivalent systems to treat pathologies mediated by carbohydrate-lectin interactions.[127] For example, it has been recognized that selectins and sialoadhesins play an important role as receptors in common biological processes and pathologies such as cell adhesions, inflammations, thrombosis, tumour cell metastases and pathogen infections by means of protein-carbohydrate binding. Synthetic compounds blocking these processes have the potential to be used in the so-called anti-adherent therapy, a particularly relevant alternative to antibiotics that are prone to bacterial resistance.[92] On the other hand, efficient and simple methods for the detection of lectins are of high and current importance, as there are some natural toxins such as Ricin, Boutulinum toxin, and E. coli toxin, among others, which are highly toxic.[128] To confidently address these problems with our system, a prerequisite condition is that the glycoligands are well disposed on the nanoconstructs surface to interact with their receptors. To this end, we exploited the known selective recognition of sugars by lectins.[129-130] The peanut agglutinin lectin (PNA) from *Arachis hypogaea* was shown to specifically interact with lactose epitopes, while concanavalin A (ConA), a lectin obtained from jack bean (*Concavalis ensiformis*) is known to selectively recognize α-mannopyranoside, α-glucopyranoside and to a lesser extent, α-*N*-acetylglucosamine, but not β-lactose.[131-132]

Mixing lactose-coated nanotubes SWCNT-**4** with PNA in Hepes buffer at pH 7.4 induced the disappearance of shish kebab-like topology of the aggregate and the characteristic striations could not be observed anymore. Instead, the TEM image shows that PNA covered extensively the functionalized nanotubes whose surface becomes fuzzy and from which individual lectin molecules can be found to stick out, Figure 6A. The same results were obtained after incubation of mannose coated glyconanotubes SWCNT-**6** with Con A, Figure 6B, where the bound protein on the tube surface mask the regular striations.

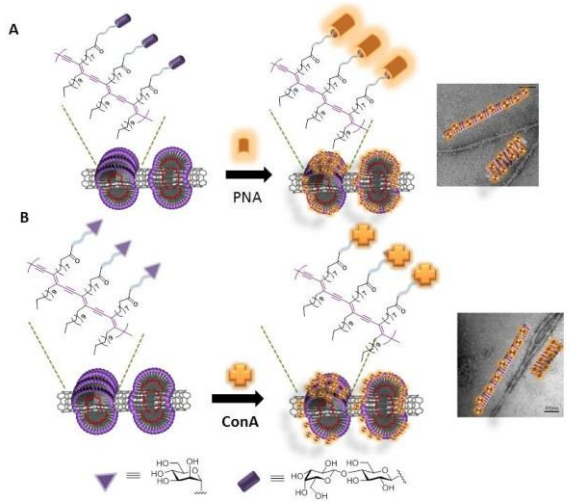

Figure 6. Schematic representation and TEM images characterization of the specific interaction with lactose coated glyconanotubes SWCNTs-**4** with PNA lectin (A), and mannose coated glyconanotubes SWCNTs-**6** ... concanavalin A (B).

The sizes of the particles attached to the SWCNTs-**4** were measured when they could be clearly delineated at the edges of the tubes (see supplementary material). In the case of PNA-SWCNT-**4** nanohybrid**,** a value of 70 Å was obtained (σ = 8 Å, n =13) which is consistent with the size of the 110 kDa PNA homotetramer for which a hydrodynamic radius of 39 Å was determined by ultracentrifugation analysis and dynamic light scattering (DLS). On the contrary, neither the mixing of CNT-**4** with ConA, nor CNT-**6** with PNA caused the disappearance of the shish-kebab topology. Both experiments gave visible regular striations around the SWCNT surfaces, figure 7 B and 7D, indicating that SWCNTs coated with glyconanorings can engage specific molecular recognition bind protein receptors and preclude non-specific protein binding.

Interestingly, the results reported herein constitute a simple and straightforward method for detecting the presence or absence of a given lectin (or toxin) in the medium. After TEM analysis, the disappearance of striation in the TEM grid indicates the presence of the sought lectin, while the observation of the shish kebab topology indicates its absence. Figure 7.

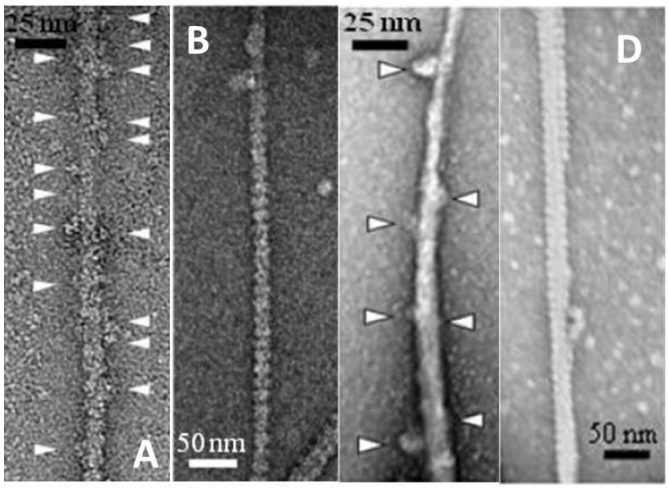

Figure 7. TEM images of glyconanotubes/lectins interactions. SWCNT-**4**/PNA interaction (A) SWCNT-**4**/ConA interaction (B). SWCNT-**6**/ConA interaction (C). SWCNT-**6**/PNA interaction (D). White arrows show the lectins protuberance at the edge of SWCNT-aggregates.

2.5 Cellular biocompatibility of functionalized SWCNTs

The key factors that influence further developments of engineered SWCNTs for biological applications are first related to cellular biocompatibility, which is a relevant concern in the field.[43-45] In this sense, toxicity of SWCNTs is primary linked to water insolubility of the pristine material, and secondarily to the surface chemistry modifications carried out to render it soluble.[42] We therefore wanted to consider whether our hybrid method for the synthesis of water soluble CNTs based on multivalent display of saccharide epitopes is affecting key parameters related to cellular biocompatibility. For that purpose, and as a proof of concept, we used a well-established cell line,[133] and a similar approach[134] to understand the biological outcome of the interaction between cells and nanoparticles in order to analyze cell membrane integrity, cell growth kinetics and cell cycle after SWCNT-**6** exposure (Figure 8).

RAW 264.7 cells were treated for 24 h with different concentrations of either SWCNTs or SWCNTs-**6** and extracellular LDH release was measured as a surrogate marker of membrane integrity (Figure 8A).[135] While unmodified SWCNTs impaired membrane integrity, cells exposed to either 10 or 50 μM SWCNTs-**6** showed reduced levels of LDH, consistent with no toxicity. The LDH reduction over control values for SWCNTs-**6** is in agreement with a slight reduction in cell proliferation rates without affecting cell viability. Cell membrane integrity after exposure of either SWCNTs or SWCNTs-**6** was also monitored as the ability of living cells to exclude intracellular access of propidium iodide (PI) evaluated by flow cytometry (FACS) (Figure 8B).

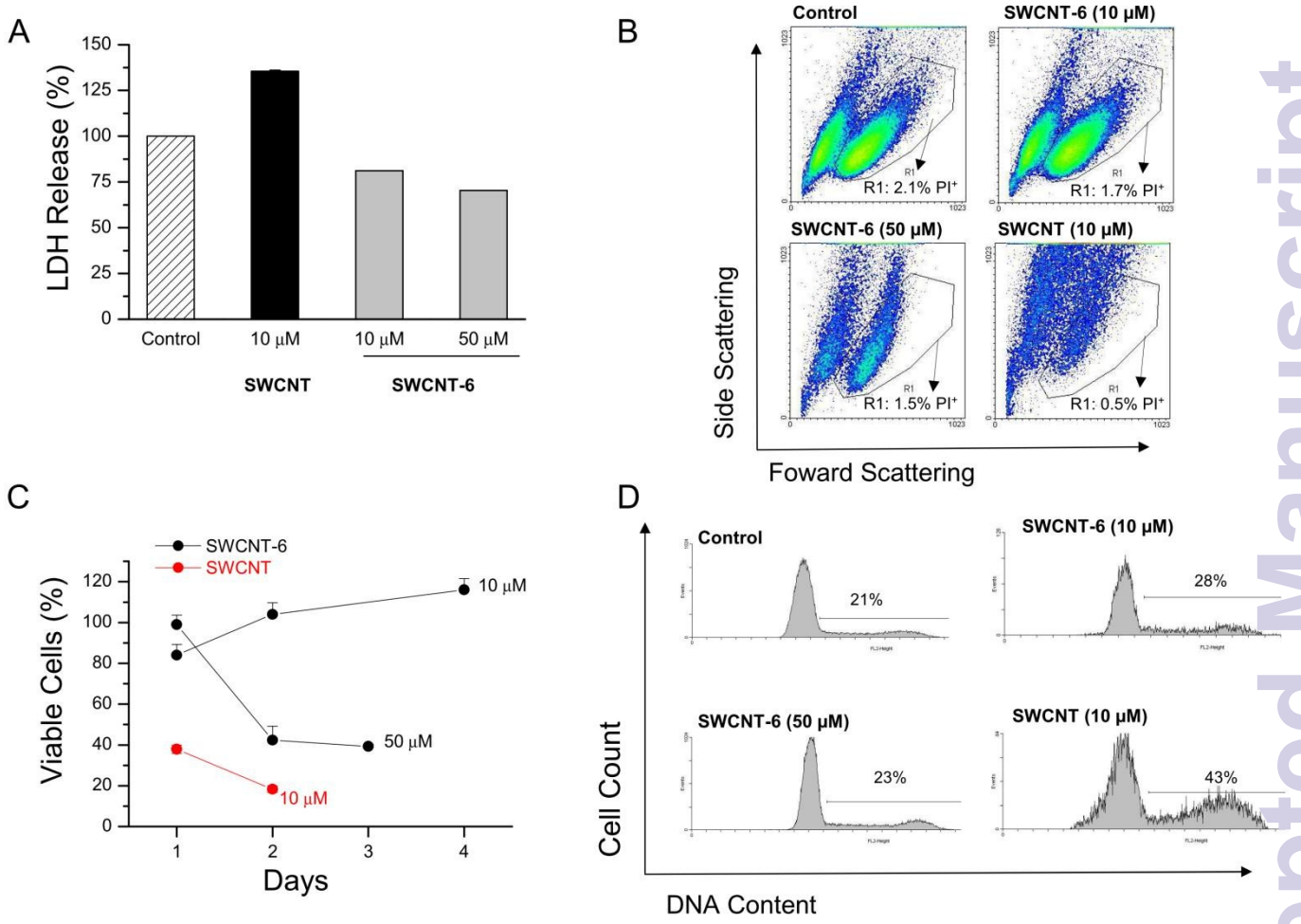

Figure 8. Effect of SWCNTs functionalization on cell biocompatibility. Cytotoxicity was determined by LDH assay of RAW 264.7 cells as readout of cell membrane integrity of cells incubated for 24 h in the absence or presence of either SWCNTs or SWCNTs-**6** at different concentrations (A), and by FACS analysis of cells treated under the same conditions after PI staining (B). FACS plots shown FS vs SS patterns of RAW 264.7 cells under the different treatments, indicating the percentage of dead cells (PI positive) inside the R1 region. Cell growth kinetic studies of RAW 264.7 in the absence or presence of either SWCNTs or SWCNTs-**6** at different concentrations measured by trypan-blue negative cell counting under light microscopy, expressed as the percentage of viable cells compared to untreated cell cultures for a given day (C). Cell cycle analysis by FACS showing DNA content in RAW 264.7 cells treated for 24 h in the absence or presence of either SWCNTs or SWCNTs-6 at different concentrations. The M1 region shows the percentage of cells in S and G2/M cell cycle phases (D).

In agreement with our previous observations, there was no increase in the percentage of dead cells after treatment with SWCNT-**6** at either 10 μM or 50 μM concentrations. Nevertheless, a clear alteration in the light scattering properties was observed for the SWCNT treated cells, suggesting a remodelling in the cell morphology driven by SWCNTs exposure (Figure 8B; right bottom panel). This effect was not appreciated for SWCNTs-**6** exposure, even though a scanty outcome was observed for the high dose of SWCNTs-**6**. On the contrary, SWCNTs exposure resulted in an increase in the number of dead cells (PI positive) in the non-R1 region, although the levels of PI exclusion were similar to those untreated for or SWCNTs-**6** treated cells (Figure 8B). We next evaluated the cell growth kinetics over a period of 4 days exposure to either SWCNTs or SWCNTs-**6** compared to untreated cells. Figure 8C shows the number of viable cells, expressed as the percentage of the viable cells from non-treated cultures. While cells exposed to 10 μM SWCNTs-**6** grew at the same rate that control cells during the 4 days of culture, the effect of SWCNTs was evident at day 1. Remarkably, the cell cycle assessment carried out by FACS analysis of the DNA content indicated that the effects of SWCNTs are mainly mediated by an arrest of the cell cycle in the G2/M phase (Figure 8D)

Conclusions

In this work, we have reported a hybrid method for the functionalization and water dispersion of SWCNTs, which combines the advantages of covalent and non-covalent currently used. The method is based on the hierarchical self-organization of diacetylenic based neoglycolipids on the CNT sidewalls. Preliminary mechanistic studies have shown that the optimal neoglycolipid type **I** first self-organizes into micelles in aqueous solution, and then undergoes a hemi-micellar arrangement on the solid surface of the CNTs. Interestingly, TEM and AFM analyses showed that compounds type **I** self-

assemble on the SWCNT surfaces in a supramolecular fashion, resulting in rings made of rolled-up half cylinders. The photo-polymerization of the diacetylene function upon UV irradiation (254 nm) affords a conjugated polydiacetylene backbone of alternating enyne groups which rigidifies the inner core of each hemi-micelle, resulting in robust polymerized glyconanorings around the nanotube in a shish-kebab topology. The UV-Vis-NIR analysis together with Raman spectroscopy shows that the functionalization takes place without perturbing the electronic nature of the nanotube surface. Anthrone method coupled with thermogravimetric analysis demonstrates the high degree of coverage of the nanotube surface with the sugar epitope. The carbohydrates on the glyconanotube surface are able to establish selective interactions with specific lectins as shown by a simple analysis with the transmission electronic microscope.

Remarkably, the cellular interaction of functionalized SWCNTs demonstrated a biocompatible profile suitable for further biological experimentation. In this sense, our glyconanotubes produced a minor decrease in cell proliferation rates without affecting cell viability in terms of membrane integrity, cell growth kinetics over long periods of exposure and cell cycle studies. It is worth to mention that pristine SWCNTs mainly impair cell cycle, leading to an arrest in the G2/M phase instead of having a major direct effect on membrane integrity. The latter highlights the need to perform multiple and complementary biological tests to better understand the biological interplay between cells and CNTs.

The results reported herein highlight the potential of the formed glyconanotubes as nanometric multivalent inhibitors of pathologic events taking place through carbohydrate-lectin interactions, such toxins, viruses and bacteria infections. Moreover, combining the glyconanotube specific lectin interactions with appropriate read-out transducers, can lead to sensor devices suitable for detecting toxins and bacteria in food, water, as well as in clinical settings and chemical and biological warfare scenarios.

4 Experimental

4.1 General procedure for amide formation with 10,12-pentacosadiyonic acid

TBTU (0.2 M, 1 eq) and DIPEA (1.5 eq) were added sequentially at room temperature to a solution of the PCDA (0.2 M, 1 eq) in DMF. The solution was stirred for 5 min, then a solution of the corresponding amino derivative (0.2 M, 1 eq) and DIPEA (1.5 eq) in DMF was added slowly. The solution was stirred for 14 h before the solvent was removed under vacuum. The residue was dissolved in CH_2Cl_2 (200 mL) and washed with 1 M HCl (40 mL), saturated aqueous $NaHCO_3$ (60 mL) and brine (40 mL). After drying over Na_2SO_4 and removal of solvent, the crude product was purified by silica gel chromatography eluting with CH_2Cl_2/MeOH (20:1).

General procedure for amide formation with the spacer

TBTU (1 eq.) and DIPEA (1.5 eq.) were added sequentially at room temperature to a solution of the spacer (0.2 M, 1 eq.) in DMF. The solution was stirred for 5 min, then a solution of the corresponding amino derivative (1 eq.) and DIPEA (1.5 eq.) in DMF (0.2 M) was added slowly. The solution was stirred for 14 h before the solvent was removed under vacuum. The residue was dissolved in CH_2Cl_2 (200 mL) and washed with 1M HCl (40 mL), saturated aqueous $NaHCO_3$ (60 mL) and brine (40 mL). After drying over Na_2SO_4 and removing of solvent, the crude product was purified by silica gel chromatography eluting with CH_2Cl_2/MeOH (20:1).

4.2 General procedure for the synthesis of free glycolipids by Zemplen deacetylation:

NaOMe (0.1 eq /acetate group) in MeOH was added to a solution of per-O-acetylated glycolipid (0.02 M, 1 eq). The reaction was allowed to proceed at room temperature for 1h, at which time the reaction was judged complete by TLC analysis. A sufficient quantity of Amberlyst Ir-120 (plus) (H form) resin was added to the mixture to render the pH of the solution neutral. The resin was removed by filtration and the solvent removed under vacuum. The crude product was purified by size-exclusion chromatography (Sephadex G20) eluting with methanol.

4.3 General procedure for the functionalisation of SWCNTs with photo-polimerisable glycolipids derivatives.

SWCNTs were purchased from Carbon Solutions Company. In a typical experiment, 1 mg of glycolipid is dissolved in 1 ml of milliQ water, and then 1 mg of SWCNT was added to the homogenous solution. The mixture was sonicated using a simple ultrasound waterbath for 1 h. Insoluble material and impurities (amorphous carbon and metallic catalyst) were then removed by low-speed centrifugation at 825 x g for 4 min. After that, the stable black aqueous solution of functionalized glycolipid-SWCNT was irradiated by a UV lamp at 254 nm for 24h to initiate and complete the photo-polymerization of the di-yne function to polydiacetylene. A second high-speed centrifugation at 17968 x g for 10 min was then performed for the sedimentation of the stable polymerized functionalized glycolipid-SWCNT and the elimination of excess glycolipids (micelles) which remains in the supernatant solution. This process was repeated four times to remove the excess of the glycolipids.

4.4 Determination of carbohydrate quantity by anthrone method.

A freshly prepared solution of anthrone (0.5 % w/v in concentrated H_2SO_4, 1 mL) was added to various concentrations of D-mannose and lactose of known concentration (0.5 mL) under stirring in a water-bath. After that, the solution was then heated at 90ºC for 12 min. Then the resulting green bluish solutions were rapidly cooled down in an ice bath during a further 10 min. Next, the absorbance of the solution was measured at 620 nm and the data were plotted against D-mannose and lactose concentrations obtaining the calibration curves for each sugar. To calculate the carbohydrate quantity on SWCNTs, 0.5 mg of SWCNTs-Lac and 1.15 mg of SWCNTs-Man were dissolved in 0.5 mL Milli-Q water, and then a freshly prepared solution of anthrone was added, following the same procedure described above.

4.5 General procedure for determining the specific interaction between glycolipid-SWCNT aggregates and lectins (PNA and Con A).

A 100 µL stable aqueous solution of glycolipid-SWCNs was incubated for 1h at room temperature in presence of lectin solution (20 mM Hepes aqueous buffer at pH =7.5). The mixture was centrifuged at low speed, and 10µL of the result aggregation was drop casting on carbon coated grid. After 2 min adsorption the sample was negatively stained with a 2% (w/v) uranyl acetate solution and observed by TEM microscopy.

4.6 Cell viability assays.

The Raw 264.7 mouse cell line was obtained from ECACC (Porton Down, Wiltshire, UK). The cells were maintained in RPMI 1640 medium (BioWhittaker) supplemented with 10 % fetal bovine serum (BioWhittaker), 1% L-glutamine, 100 IU/mL penicillin and 100 IU/mL streptomycin (BioWhittaker) in a humidified atmosphere of 5 % CO2 at 37 °C.

SWCNTs were dissolved in DMSO while functionalized SWCNTs-**6** were dissolved in water, both at concentrations of 1 mM as stock solutions (equivalent to 1.25 mg/ml). The SWCNTs stock solution was added dropwise into RPMI culture medium using an ultrasound water bath to achieve efficient dispersion of the material at working concentrations ranging from 10 µM to 50 µM of SWCNTs. Final concentrations of SWCNTs-**6** were referred to the concentration of the glycolipid while pristine SWCNTs concentrations were referred to the corresponding nanoparticles as determined by TGA.

Extracellular LDH release from adherent cell cultures was determined following previous report with minor modifications.[127] Raw 264.7 cells were seeded in 96-well plates at a density of 40000 cells per well, in a final volume of 200 µL of complete RPMI 1640 medium as indicated above. After overnight incubation, the supernatants were replaced with fresh complete media containing different concentrations of SWCNTs or SWCNTs-**6** and incubated for 24 hours. Then, LDH release was determined in the supernatant of each well according to manufacturer's instructions (Roche Diagnostics GmbH, Mannheim, Germany). Spectrophotometric absorbances were determined using a microplate (ELISA) reader at 570 nm with 660 nm as reference wavelength. LDH release was expressed as the percentage of the LDH release from untreated RAW 264.7 cell cultures under the same conditions. Each experimental condition was performed in triplicate.

For determination of cell apoptosis and cell cycle analysis, adherent RAW 264.7 cells were seeded overnight in 24-well plates at a density of 170.000 cells per well, and cultured in a final volume of 1 mL of complete RPMI 1640 medium. The following day the supernatants were replaced with 1 mL of complete RPMI 1640 fresh media in the absence or presence of either SWCNTs or SWCNTs-**6** at different concentrations and incubated for 24 hours. Thereafter, cells were trypsinized and washed with PBS for subsequent cell apoptosis and cell cycle studies. For detection of apoptotic cells, cells were resuspended in PBS containing 1% (v/v) fetal bovine serum and 10 µg/mL of propidium iodide (PI), and further incubated for 15 minutes in the dark. PI exclusion of FS/SS cells was determined by flow cytometry (FACS) (Becton Dickinson). Cell cycle analysis was analyzed by measuring the DNA content. RAW 264.7 cells (10^6 cells) were fixed in ice-cold solution of 70% ethanol for at least 24h, and then incubated with 0.1% (w/v) RNAse and 50 µg/mL of PI at 37 ºC for 30 min before analysis for DNA content by flow cytometry using cell quest software.

For cell growth kinetic studies, Raw 264.7 cells were seeded overnight in 24-well plates at a density between 100.000 and 200.000 cells per well, and cultured for 1 to 4 days in the absence or presence of different concentrations of SWCNTs or SWCNTs-**6**, including a medium change every other day. Cells were trypsinized and counted by trypan-blue exclusion under light microscopy at different time points

Acknowledgements

Financial support was provided by the Andalusian Ministry of Economy, Science and Innovation (P10-CTS-6928 and P11-CTS-8161 to DP; P07-FQM-2774 to NK, P11-FQM-8046 to IF), the PAIDI Program from the Andalusian Government (CTS-677 to DP; FQM-102 to IF), the Spanish Ministry of Economy and Competitiveness (CTQ2013-49066-C2-1-R to NK and PI14-1600 to DP). MA holds a MAEC-AECID PhD fellowship. JJC holds a JAE-CSIC postdoctoral fellowship. We thank the Centre for Research Technology and Innovation of the University of Seville (CITIUS) for the use of TEM, AFM, and NMR facilities.

Notes and references

1 S. Ijima, *Nature* 1991, **354**, 56–58
2 S. Ijima, T. Ichihashi, *Nature* 1993, **363**, 603-605.
3 P. J. F. Harris, in *Carbon nanotube science-synthesis, properties, and applications*. Cambridge Univ. Press, Cambridge, 2009.
4 J. M. Schnorr, T. M. Swanger, *Chem. Mater.* 2011, **23**, 646-647.
5 R. H. Baughman, A. A. Zakhidov, W. A. C. de Heer, *Science* 2002, **297**, 787-792.
6 M. F. L. De Volder, S. H. Tawfick, R. H. Baughman, A. J. Hart, *Science* 2013, **339**, 535-539.
7 N. K. W. Kam, T. C. Jessop, P. A. Wender, H. J. Dai, *J. Am.Chem. Soc.* 2004, **126**, 6850-6851.
8 X. Shi, A. von dem Bussche, R. H. Hurt, A. B. Kane, H. Gao, *Nat. Nanotechnol*. 2011, **6**, 714-719.
9 C. Fabbro, H. Ali-Boucetta, T. Da Ros, K. Kostarelos, A. Bianco, M. Prato, *Chem Commun.* 2012, **48**, 3911-26.
10 C. Cha, S. R. Shin, N. Annabi, R. Mehmet, M. R. Dokmeci, A. Khademhosseini, *ACS Nano* 2013 , **7** , 2891-2897.
11 S. K. Vashist, D. Zheng, G. Pastorin, K. Al-Rubeaan, J. H. T. Luong, F. S. Sheu, *Carbon* 2011, **49**, 4077-4097.
12 W. Yang, K. R. Ratinac, S. P. Ringer, P. Thordarson, J. J. Gooding, F. Braet, *Angew. Chem. Int Ed.* 2010, **49**, 2114-2138.
13 W. Nakanishi, K. Minami, L. K. Shrestha, Q. Ji, J. P. Hill, K. Ariga, *Nano Today* 2014, **9**, 378-394.
14 E. Heister, V. Neves, K. Lipert, H. M. Coley, S. R. Silva, J. McFadden. *Carbon* 2009, **47**, 2152-2160.

15 X. Zhang, L. Meng, Q. Lu, Z. Fei, P. J. Dyson, *Biomaterials* 2009, **30**, 6041-6047.
16 J. Chen, S. Chen, X. Zhao, L. V. Kuznetsova, S. S. Wong, I. Ojima, *J. Am. Chem. Soc.* 2008, **130**, 16778-16785.
17 S. Dhar, Z. Liu, J. Thomale, H. J. Dai, S. J. Lippard, *J. Am. Chem. Soc.* 2008, **130**, 11467-11476.
18 Z. Liu, X. Sun, N. Nakayama-Ratchford, H. J. Dai, *ACS Nano* 2007, **1**, 50-56.
19 Z. Liu, K. Chen, C. Davis, S. Sherlock, Q. Cao, X. Chen, H. J. Dai, *Cancer Res.* 2008, **68**, 6652-6660.
20 Z. Zhang, X. Yang, Y. Zhang, B. Zeng, S. Wang, T. Zhu, R. B. Roden, Y. Chen, *Clin. Cancer Res.* 2006, **12**, 4933-4939.
21 J. E. Podesta, K. T. Al-Jamal, M. A. Herrero, B. Tian, H. Ali-Boucetta, V. Hegde, A. Bianco, M. Prato, K. Kostarelos, *Small* 2009, **5**, 1176-1185.
22 J. Qiao, T. Hong, H. Guo, Y. Q. Xu, D. H. Chung, in *NanoBiotechnology Protocols*. Springer: Springer; 2013:137.
23 A. A. Bhirde, V. Patel, J. Gavard, G. Zhang, A. A. Sousa, A. Masedunskas, R. D. Leapman, R. Weigert, J. S. Gutkind, J. F. Rusling, *ACS Nano* 2009, **3**, 307-316.
24 M. R. McDevitt, D. Chattopadhyay, B. J. Kappel, J. S. Jaggi, S. R. Schiffman, C. Antczak, J. T. Njardarson, R. Brentjens, D. A. Scheinberg, *J. Nucl. Med*. 2007, **48**, 1180-1189.
25 A. Star, E. Tu, J. Niemann, J-C. G. Gabriel, C. S. Joiner, C. Valcke, *Proc. Natl. Acad. Sci. U.S.A.* 2006**, 103**, 921-926.
26 E. S. Snow, F. K. Perkins, E. J. Houser, S. C. Badescu, T. L. Reinecke, *Science* 2005, **307**, 1942-1945.
27 S. Y. Hong, G. Tobias, K. T. Al-Jamal, B. Ballesteros, H. Ali-Boucetta, S. Lozano-Perez, P. D. Nellist, R. B. Sim, C. Finucane, S. J. Mather, M. L. H. Green, K. Kostarelos, B. J. Davis, *Nat. Mater.* 2010, **9**, 485-490.
28 K. Sahithi, M. Swetha, K. Ramasamy, N. Srinivasan, N. Selvamurugan, *Int. J. Biol. Macromol.* 2010, **46**, 281-283.
29 S. R. Shin, H. Bae, J. M. Cha, J. Y. Mun, Y. C. Chen, H. Tekin, H. Shin, S. Farshchi, M. R. Dokmeci, S. Tang, A. Khademhosseini. *ACS Nano* 2012, **6**, 362.
30 S. R. Shin, S. M. Jung, S. Zalabany, K. Kim, P. Zorlutuna, S. B. Kim, M. Nikkhah, M. Khabiry, M. Azize, J. Kong, K. T. Wan, T. Palacios, M. R. Dokmeci, S. Tang, A. Khademhosseini. *ACS Nano* 2013, **7**, 2369-2380.
31 Y. Liu, Y. Zhao, B. Sun, C. Chen, *Acc. Chem. Res*. **2013**, *46*, 702-713.
32 S. T. Yang, J. Luo, Q. Zhou, H. Wang, *Theranostics* 2012, **2**, 271-282.
33 C. W. Lam, J. T. James, R. McCluskey, S. Arepalli, R. L. Hunter, R. L. *Crit. Rev. Toxicol*. 2006, **36**, 189-217.
34 C. P. Firme, P. R. Bandaru, *Nanomed. Nanotechnol. Biol. Med*. 2010, **6**, 245-256.
35 Y. Sato, A. Yokoyama, K. I. Shibata, Y. Akimoto, S. I. Ogino, Y. Nodasaka, T. Kohgo, K. Tamura, T. Akasaka, M. Uo. *Mol. BioSyst*. 2005, **1**, 176-182.
36 P. Wick, P. Manser, L. K. Limbach, U. Dettlaff-Weglikowska, F. Krumeich, S. Roth, W. J. Stark, A. Bruinink. *Toxicol. Lett.* 2007, **168**, 121-131.
37 C. Poland, R. Duffin, I. Kinloch, A. Maynard, W. Wallace, A. Seaton, V. Stone, S. Brown, W. Macnee, K. Donaldson. *Nat. Nanotechnol*. 2008, **3**, 423–428.
38 G. M. Mutlu, G. R. S. Budinger, A. A. Green, D. Urich, S. Soberanes, E. Sergio, S. E. Chiarella, G. F. Alheid, D. R. McCrimmon, I. Szleifer, M. C. Hersam, *Nano Lett.* 2010, **10**, 1664-1670.
39 Z. Liu, C. Davis, W. Cai, L. He, X. Chen, H. J. Dai, *Proc. Natl. Acad. Sci. USA* 2008, **105**, 1410-1415.
40 M. L. Schipper, M. N. Nakayama-Ratchford, C. Davis, N. K. W. Kam, P. Chu, Z. Liu, X. Sun, H. J. Dai, *Nature Nanotech*. 2008, **3**, 216-221.
41 R. Singh, D. Pantarotto, L. Lacerda, G. Pastorin, C. Klump, M. Prato, K. Kostarelos, A. Bianco. *Proc. Natl. Acad. Sci. USA* 2006, **103**, 3357-3362.
42 H. Ali-Boucetta, A. Nunes, R. Sainz, M. A. Herrero, B. Tian, M. Prato, A. Bianco, K. Kostarelos, *Angew. Chem. Int. Ed*. 2013, **52**, 2274 –2278.
43 H. C. Wu, X. Chang, L. Liu, F. Zhao, Y. Zhao, *J. Mater. Chem.* 2010**, 20**, 1036-1052.
44 A. Bianco, K. Kostarelos, M. Prato, *Chem. Commun.* 2011, **47**, 10182.
45 A. Battigelli, C. Ménard-Moyon, T. Da Ros, M. Prato, A. Bianco, *Adv. Drug Deliv.* 2013, **65**, 1899-1920.
46 N. Karousis, N. Tagmatarchis, D. Tasis, *Chem. Rev*. 2010, **110**, 5366-5397.
47 P. Singh, S. Campidelli, S. Giordani, D. Bonifazi, A. Bianco, M. Prato, *Chem. Soc. Rev*. 2009, **38**, 2214-2230.
48 X. Peng, S. S. Wong, *Adv. Mater.* 2009, **21**, 625-642.
49 D. A. Britz, A. N. Khlobystov, *Chem. Soc. Rev.* 2006*,* **35**, 637–659.
50 U. Hahn, S. Engmann, C. Oelsner, C. Ehli, D. M. Guldi, T. Torres, *J. Am. Chem. Soc.* 2010, **132**, 6392-6401.
51 Y. Lee, K. E. Geckeler, *Adv. Mater*. 2010**, 22**, 4076-4083.
52 Y. L. Zhao, J. F. Stoddart, *Acc. Chem. Res*. 2009, 42, 1166-1171.
53 M. Assali, M. Pernia Leal, I. Fernández, R. Baati, C. Mioskowski, N. Khiar, *Soft Matter* 2009, **5**, 948-950.
54 M. Assali, M. Pernia Leal, I. Fernández, P. Romero-Gómez, R. Baati, N. Khiar, *Nano Research* 2010, **3**, 764-778.
55 P. Wu, X. Chen, N. Hu, U. C. Tam, O. Blixt, A. Zettl, C. R. Bertozzi, *Angew. Chem. Int. Ed*. **2008**, *47*, 5022 –5025
56 H. G. Sudibya, J. Ma, X. Dong, S. Ng, L-J. Li, X-W. Liu, P.Chen, *Angew. Chem. Int. Ed.* **2009**, *48*, 2723-2726
57 G. Clavé, G. Delport, C. Roquelet, J. S. Laurent, E. Deleporte, F. Vialla, B. Langlois, R. Parret, C. Voisin P. Roussignol, P. Jousselme, A. Gloter, O. Stephan, A. Filoramo, V. Deryke, S. Campidelli, *Chem. Mater.* 2013, **25**, 2700-2707.
58 R. Liu, X. Zeng, J. Liu, Y. Zheng, J. Luo, X. Liu, *J. Mater. Chem. A.* 2004, **2**, 14481-14483.
59 G. M Whitesides, J. P. Mathias, C. T. Seto, *Science*, 1991, **254**, 1312-1319.
60 J. M. Lehn, *Science* 2002, **295**, 2400-2403.
61 G. M. Whitesides, *Small* 2005, **1**, 172-179.
62 G. Z. Wegner, *Naturforsch, B: Anorg. Chem. Org. Chem. Biochem. Biophys. Biol*., 1969, **24b**, 824-827.
63 D. Day, H. J. Ringsdorf, *Polym. Sci., Polym. Lett. Ed.,* 1978, **16**, 205-210.
64 M. A. Reppy, B. A. Pindzola, *Chem. Commun.,* 2007, 4317-4338.
65 J. W. Lauher, F. W.; Fowler, N. S. Goroff, *Acc. Chem. Res.* 2008, **41**, 1215-1229.
66 B. Yoon, S. Lee, J. M. Kim, *Chem. Soc. Rev.,* 2009, **38**, 1958-1968.
67 X. Sun, T. Chen, S. Huang, L. Li, H. Peng, *Chem. Soc. Rev.* 2010, **39**, 4244-4257.
68 O. Yarimaga, J. Jaworski, B. Yoon, J. –M. Kim, *Chem. Commun.* 2012, **48**, 2469-2485.
69 M. Pernía Leal, M. Assali, I. Fernández N. Khiar, *Chem.–Eur. J*., 2011, **17**, 1828-1836.
70 E. Contal, A. S. Klymchenko, Y. Mély, S. Meunier, A. Wagner, *Soft Matter*, 2011, **7**, 1648-1650.
71 H. Jiang, X. J. Pan, Z. Y. Lei, G. Zou, Q. J. Zhang, K. Y. Wang, *J. Mater. Chem.,* 2011, **21**, 4518-4522.
72 W. Zhou, Y. Li, D. Zhu, *Chem. Asian J.* 2007, **2**, 222-229.
73 M. Assali, J. J. Cid; I. Fernández, N. Khiar, *Chem. Mater*. 2013, **25**, 4250-4261.
74 N. Khiar, M. Pernia Leal, R. Baati, C. Ruhlmann, C. Mioskowski, P. Schultz, I. Fernández, *Chem. Comm.* 2009, 4121-4123.

75 M. Assali, M. Pernía-Leal, I. Fernández, N. Khiar, *Nanotechnology*, **24** (2013) 085604.
76 M. Assali, J. J. Cid, M. Pernia Leal, M. Muñoz-Bravo, I. Fernández, R. E. Wellinger, N. Khiar, *ACS Nano* 2013**, 7**, 2145-2153.
77 O. Kharissova, B. I. Kharisov, E. G. de Casas Ortiz, *RSC Adv.* 2014, **3**, 24812-24852.
78 T. Premkumar, R. Mezzenga, K. Geckeler, *Small*, 2012, **8**, 1299-1313.
79 M. Fagoni, P. Mustarelli, A. Profumo, E. Quartarone, D. Merli, D. Ravelli, *RSC Adv.* 2013, **3**, 13569-13582.
80 M. Calvaresi, M. Dallvalle, F. Zerbetto, *Small*, 2009, **5**, 2191-2198.
81 G. Srinivas, S. O. Nielsen, P. B. Moore, M. L. Klein, *J. Am. Chem. Soc.* 2006, **128**, 848-853.
82 J. Määttä, S. Vierros, P. R. Tassel, M. Sammalkorpi, *J. Chem. Eng. Data* 2014, **49**, 3080-3089.
83 A. J. Blanch, A. C. E. Lenehan, J. S. Quinton, *J. Phys. Chem. B* 2010, **114**, 9805-9811.
84 B. Bertels, M. Bruyninckx, M. Kurttepeli, M. Smet, S. Bals, B. Goderis, *Langmuir* 2014, **30**, 12200-12209.
85 N. K. Subbaiyan, N. S. Canbré, A. N. G. Parra-Vazquez,E. H. Hároz, S. Doorn, J. G. Duque, *ACS Nano* 2014, **8**, 1619-1628.
86 B. Capon, *Chem. Rev*., 1969, **69**, 407–498.
87 R. Roy, D. Zanini, S. J. Meunier, A. Romanowska, *Chem. Commun*., 1993, 1869–1872.
88 M. Gingras, Y. M. Chabre, M. Roy, R. Roy, *Chem. Soc. Rev*., 2013, **42**, 4823-4841.
89 K. Y. Kim, A. Varki, *Glyconcojugate J.* 1997**, 14**, 569-576.
90 X. Zeng, C. A. S. Andrade, M. D. L. Oliveira, M. X. L. Sun, *Anal. Bioanal. Chem.* 2012, **402***, 3161-3176.*
91 S. K. Wang, P. H. Liang, D. Rena, R. D. Astronomo, R. D.; T. L. Hsu, S. L. Hsieh, D. R. Burton, C. H. Wong, *Proc. Nat. Acad. Sc. USA* 2008, **105**, 1806-1809.
92 A. Bernardi, J. Jimenez-Barbero, A. Casnati, D. de Castro, T. Darbre, F. Fieschi, J. Finne, H. Funken, K. Jaeger, M. Lahmann, T. K. Lindhorst, M. Marradi, P. Messner, A. Molinaro, P.V. Murphy, C. Nativi, S. Oscarson, S. Penades, P. Peri, R. J. Pieters, O. Renaudet, J. Reymond, B. Richichi, J. Rojo, F. Sansone, C. Schaeffer, W.B. Turnbull, T. Velasco-Torrijos, S. Vidal, S. Vincent, T. Wennekes, H. Zuilhof, A. Imberty, *Chem. Soc. Rev*., 2013, **42**, 4709-4727.
93 O. Martínez-Avila, L. M. Bedoya, M. Marradi, C. Clavel, J. Alcamí, S. Penadés, *ChemBioChem.* 2009, **10**, 1806-1809.
94 J. E. Hudak, C. R. Bertozzi, *Chem Biol.* 2014, **21**, 16-37.
95 J. C. Manimala, T. A. Roach, Z. Li, J. C. Gildersleeve, *Angew. Chem. Int. Ed*. 2006, **45**, 3607-3610.
96 F. Fazio, M. C. Bryan, O. Blixt, J. C. Paulson, C. H. Wong, *J. Am. Chem. Soc*. 2002, **124**, 14397-14402.
97 Azidoethanol is potentially explosive, and should be manipulated with caution
98 Z. Wang, *Zemplén Deacetylation.* in *Comprehensive Organic Name Reactions and Reagents.* - John Wiley & Sons, Inc. 2010, Hoboken, NJ.
99 R. Jennifer, J. R. Allen, J. G. Allen, X. F. Zhang, L. J. Williams, A. Zatorski, G. Ragupathi, O. Philip P. O. Livingston, S. J. Danishefsky, *Chem. Eur. J*. 2000, **6**, 1366-1375.
100 F.AW. Koeman, J. W. G. Meissner, H. R. P. van Ritter, J. P. Kamerling, J. F.G Vliegenhart, *J. Carbohydr. Chem*. 1994, **13**, 1-25.
101 L. Röglin, E. H. M. Lempens, E. W. Meijer, *Angew. Chem. Int. Ed*. 2011, **50**, 102-112.
102 Y. Y. Cheng, L. B. Zhao, Y. W. Li, T. W. Xu, *Chem Soc Rev.* 2011, **40**, 2673-2703.
103 A. R. Menjoge, R. M. Kannan, D. A. Tomalia, *Drug Discover. Today* 2010, **15**, 171-185.
104 Y. Shen Q. Xu, H. Gao, N. N. Zhu, *Electrochem Commun* 2009, **11**,1329-1332.
105 X. Y. Shi, S. H. Wang, M. W. Shen, M. E. Antwerp, X. S. Chen, C. Li, E. J. Petersen, Q. G. Huang, W. J. Weber, *Biomacromolecules* 2009, **10**, 1744-1750.
106 N. N. Zhu, H. Gao, Q., Xu, Y. Q. Lin, L. Su, L. Q. Mao, *Biosens Bioelectron.* 2010, **25**, 1498-1503.
107 A. J. M. Sliedregt, P. Rensen, E. T. Rump, P. J. van Santbrink, M. K. Bijsterbosch, A. Valentijn, G. A. van der Marel, J. H. van Boom, T. van Berkel, E. Biessen, *J. Med. Chem*. 1999, **42**, 609-618.
108 A. J. Blanch, C. E. Lenehan, J. S. Quinton, *Carbon* 2011 **49**, 5213-522.
109 M. S. Strano, V. C. Moore, M. K. Miller, M. J. Allen, E. H. Haroz, C. Kittrell, R. H. Huage, R. E. Smalley, *J. Nanosci. Nanotechnol.* 2003, **3**, 81-86.
110 E. J. Wallace, M. S. P. Sansom, *Nanotechnology* 2009, **20** 045101.
111 M. Calvaresi, M. Dallavalle, F. Zerbetto, *Small* 2009, **5**, 2191-2198.
112 H. Lee, H. Kim, *J. Phys. Chem. C*. 2012, **116**, 9327-9333.
113 R. Qiao, P. C. Ke, *J. Am. Chem. Soc.* 2006, **128**, 13656-13657.
114 K. Yurekli, C. A. Mitchell, R. Krishnamoorti, *J. Am. Chem. Soc.* 2004, **126**, 9902-9903.
115 M. J. O'Connell, S. H. Bachilo, C. B. Huffman, V. C. Moore, M. S. Strano, E. H. Haroz, K. L. Rialon, P. J. Boul, W. H. Noon, C. Kittrell, J. Ma, R. H. Hauge, R. B. Weisman, R. E. Smalley, *Science* 2002, **297**, 593-596.
116 O. Matarredona, H. Rhoads, Z. Li, J. H. Harwell, L. Balzano, D. E. Resasco, *J. Phys. Chem. B* 2003, **107**, 13357-13367.
117 C. Richard, F. Balavoine, P. Schultz, T. W. Ebbesen, C. Mioskowski, *Science* 2003, **300**, 775−778.
118 M. F. Islam, E. Rojas, D. M. Bergey, A. T. Johnson, A. G. Yodh, *Nano Lett.* 2003, **3**, 269-273.
119 R. Haggenmueller, S. S. Rahatekar, J. A. Fagan, J. Chun, M. L. Becker, R. R. Naik, T. Kraus, L. Carlson, J. Kadla, P. Trulove, D. Fox, H. DeLong, Z. Fang, S. O. Kelley, J. W. Gilman, *Langmuir* 2008, **24**, 5070-5078.
120 A. Di Crescenzo, V. Ettore, A. Fontana *Beilstein J. Nanochem.* 2014, **5**, 1675-1690.
121 H. Wang. *Curr. Opin. Colloid Interface Sci*. 2009, **14**, 364-371.
122 Y. Tan, D. E. Resasco, *J. Phys. Chem. B.* 2005, **109**, 14454-14460.
123 J. L. Bahr, J. Yang, D. V. Kosynkin, M. J. Bronikowski, R. E. Smalley, J. M. Tour, *J. Am. Chem. Soc.* 2001, **123**, 6536-6542.
124 V. A Sinani, M. K. Gheith, A. A. Yaroslavov, A. A. Rakhnyanskaya, K. Sun, A. A. Mamedov, J. P. Wicksted, N. A. Kotov, *J. Am. Chem. Soc.* 2005, **127**, 3463-3472.
125 M. S. Strano, C. B. Huffman, V. C. Moore, M. J. O´Connel, E. H. Haroz, J. Hubbard, M. Miller, K. Rialon, C. Kittrell, S. Ramesh, R. H. Hauge, R. E. Smalley, *J. Phys. Chem. B*. 2003, **107**, 6979-6985.
126 M. A. Jermyn, *Anal. Biochem.* 1975, **68**, 332-335.
127 Z. J. Witczak K. A. Nieforth, *Carbohydrates in drug design* Marcel Dekker Inc., 1997, New York.
128 X. Zeng, C. A. S. Andrade, M. Oliveira, X. L. Sun, X, *Anal. Bioanal. Chem.* 2012**, 402***,* 3161-3176.
129 R. Banerjee, K. Das, R. Ravishankar, K. Suguna, A. Surolia, M. Vijayan, *J. Mol. Biol*. 1996, **259**, 281-296.
130 S. André, B. Frisch, H. Kaltner, D. L. Desouza, F. Schuber, H. J. Gabius, *Pharmaceut. Res*. 2000, **17**, 985-990.
131 H. Lis, N. Sharon, *Chem. Rev*. 1998, **98**, 637-674.
132 E. E. Simanek, G. J. McGarvey, J. A. Jablonski, C. H. Wong, *Chem. Rev.* 1998, **98**, 833-862.
133 M. Cejudo-Guillén, M. L. Ramiro-Gutiérrez, A. Labrador-Garrido, A. Díaz-Cuenca, D. Pozo, *Acta Biomater.* 2012**, 8**, 4295-4303.

134 M. Pernia Leal, S. Rivera-Fernández , J. M. Franco, D. Pozo, J. M. de la Fuente, M. L. García-Martín, *Nanoscale* 2015; **7**, 2050-2059.

135 The [SWCNT-**6**] refer to the concentration of the glycolipid in the aggregate as determined by anthrone method and the [CNT] refer to the quantity of the SWCNT at the same concentration as determined by TGA.